Heterogeneous Sources of Target Patterns in Reaction−Diffusion Systems

Andrej E. Bugrim, Milos Dolnik, Anatol M. Zhabotinsky,* and Irving R. Epstein

Department of Chemistry and Volen Center for Complex Systems, Brandeis University, Waltham, Massachusetts 02254-9110

Received: May 30, 1996; In Final Form: August 8, 1996[⊗]

We show that the rate of spontaneous formation of centers of target patterns in the Belousov−Zhabotinsky reaction−diffusion system depends strongly on the concentration of the initial reagents. Computer simulations show that the dependence can be explained by the hypothesis that small heterogeneous impurities are the sources of the target patterns.

Introduction

Chemical pattern formation has been one of the numerous domains of John Ross's successful enterprise in physical chemistry and chemical physics. We are delighted to present here a study of target pattern formation arising from local variations of the kinetic parameters in the Belousov−Zhabotinsky (BZ) reaction−diffusion system.

Target patterns (TP) have been observed in a majority of reaction−diffusion systems capable of chemical oscillations.[1−8] Several mechanisms can give rise to TP formation. The most common source of TP is a pacemaker—a small region with parameters different from those of the bulk.[6,9−12] Alternatively, TP can emerge in homogeneous systems from perturbations of certain oscillating concentrations. TP result from large-amplitude perturbations of limit cycle bulk oscillations in some reaction−diffusion models.[13,14] They also develop from finite-amplitude perturbations of a steady state in systems with a subcritical Hopf bifurcation.[15] The wave instability can be a source of TP formation arising from small concentration fluctuations.[16] TP also arise as solutions of the Ginsburg−Landau equations derived in the vicinity of the Hopf−Turing codimension-2 bifurcation.[17−19]

Most experimental studies of target patterns to date have been done in the BZ reaction−diffusion system.[1−3,6−8,20−24] In many cases, TP result from randomly situated pacemakers formed by local inhomogeneities in the system parameters. On the other hand, there are experimental data which suggest that TP can arise from fluctuations in the concentrations.[3,20−23] However, most data favor the idea that, as a rule, TP in the BZ system have a heterogeneous origin.[6,25,26] Experimental observations reveal a strong dependence of the density of TP on the concentrations of the initial reagents.[3,20,22] Vidal et al. have done a statistical study of the dependence of the density of target patterns on the concentration of sulfuric acid in the BZ system purified by filtration through a Millipore 0.22 μm filter.[20] They find that a 60% increase in $[H_2SO_4]$ results in a 115% increase in the density of sources of concentric waves. If TP in the BZ system indeed arise from heterogeneous pacemakers, then it should be possible to demonstrate that the same distribution of catalytic particles results in significantly different densities of target patterns when the initial reagent concentrations vary.

Target patterns are a major cause of instability of bulk oscillations in reaction−diffusion systems.[1,3,20,22] This seems to be true also for unstirred batch reactors, where weak convection usually takes place. It has been shown that stability of bulk oscillations in the BZ system depends strongly on the concentrations of the initial reagents. In particular, if the ratio of the bromate concentration to that of malonic acid is low, bulk oscillations are stable in the absence of stirring; if the ratio is high, bulk oscillations rapidly damp in an unstirred system.[27,28]

Here we perform an experimental and computer study of the dynamics of small heterogeneous pacemakers in the BZ reaction−diffusion system.

Experimental Section

Sodium bromate, malonic acid (Aldrich), ferrous sulfate (Fisher), and 1,10-phenanthroline (Fluka) used in the experiments were of analytical grade.

The pattern formation was studied in BZ solution layers of thickness 0.8 mm placed between two glass plates separated by a plastic spacer. The circular area filled with the solution had diameter 67 mm. The working solutions were prepared by mixing and intensive stirring of the stock solutions during 10 s. The solutions were not filtered. The following initial reagent concentrations (in M) were used: $[NaBrO_3] = 0.31$; $[CH_2(COOH)_2] = 0.3$; $[KBr] = 0.05$; $[Fe(phen)_3^{2+}] = 0.004$. The experiments were carried out at $T = 25 \pm 1$ °C.

Development of patterns was recorded with a video camera augmented with an interference filter with maximum transmission at 510 nm. The data were processed with an OPTIMAS image-analysis system (BioScan).

Experimental Results

Two different concentrations of sulfuric acid were used in experiments: $[H_2SO_4] = 0.25$ and 0.50 M. In what follows, we refer to these concentrations as the low and high acidities. The system generates bulk oscillations in both cases. We have repeated the experiments with both low and high acidities 10 times for statistical evaluation. In the experiments with low acidity the first transition from the reduced to the oxidized state occurs after the solution has been placed between the glass plates. The high acidity solution displays this first transition during stirring, just before being placed between the plates.

The development of the patterns depends strongly on the acidity. At low acidity, the first circles appear when about two-thirds of the time between the first and the second bulk transitions from the reduced to the oxidized state has elapsed (Figure 1b). The bulk transition usually engulfs the circles before they can form target patterns.

At high acidity, the circles start to appear almost immediately after the solution has been placed between the glass plates. Parts c and d of Figure 1 show the patterns at the same relative times as parts a and b, respectively. The density of patterns is much

[⊗] Abstract published in *Advance ACS Abstracts,* November 1, 1996.

S0022-3654(96)01603-6 CCC: $12.00

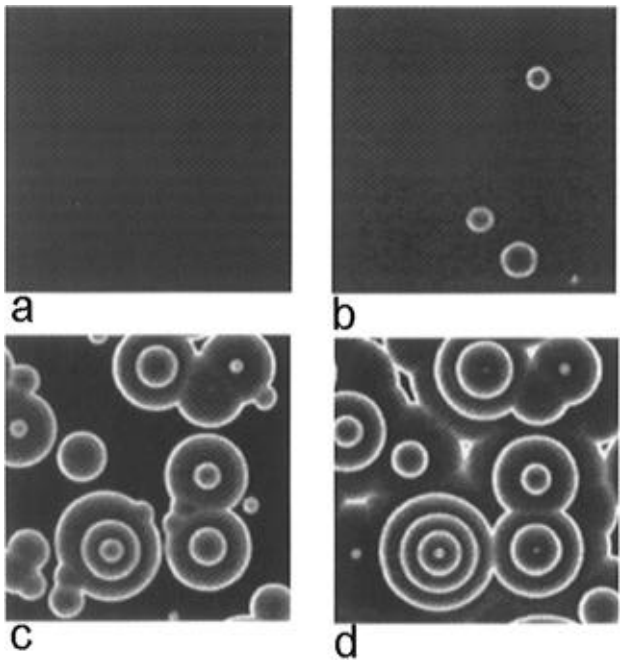

Figure 1. Target patterns in the BZ reaction−diffusion system at two different acidities. Initial reagent concentration (M): $NaBrO_3$, 0.31; $CH_2(COOH)_2$, 0.3; $Fe(phen)_3^{2+}$, 0.004. $T = 25$ °C. (a, b) $[H_2SO_4] = 0.25$ M, period of bulk oscillations $T_B = 273$ s; (c, d) $[H_2SO_4] = 0.50$ M, $T_B = 110$ s. Snapshots are taken at two equivalent time moments after the bulk transition scaled by the corresponding periods of the bulk oscillations $\tau = t/T_B$: (a, c) $\tau = 0.63$, (b, d) $\tau = 0.97$. Size of the displayed area is 40 × 40 mm.

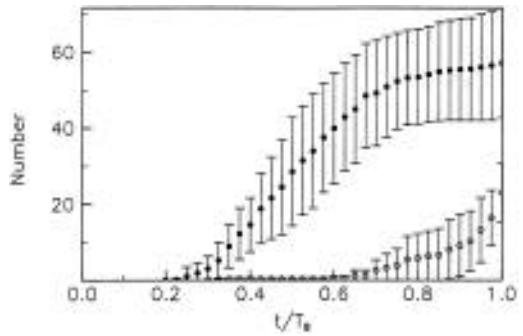

Figure 2. Appearance of circular waves in the BZ reaction−diffusion system-experiments. Cumulative plot for low acidity ($[H_2SO_4] = 0.25$ M, empty circles) and high acidity ($[H_2SO_4] = 0.50$ M, solid circles). Standard deviations are shown by error bars and are evaluated from sets of 10 experiments for each acidity.

higher at higher acidity. The circles that appear first have significantly higher frequency than the bulk oscillations, and in most cases they give rise to target patterns. The circles that appear later interact with the higher frequency target patterns or, in some cases, with the bulk transition and usually do not form target patterns.

The kinetics of generation of the circles is shown in Figure 2 as a cumulative plot of the total number of circles emerging during one period of bulk oscillation. The time is scaled by the corresponding periods of bulk oscillation, $\tau = t/T_B$, in order to compare the rate of appearance of circles for the two acidities. The high acidity curve exhibits saturation as τ approaches 1, because at this time most of the reactor is occupied by waves (Figure 1c,d). In the case of low acidity, in contrast, a significant part of the reactor is free of waves at the time of the second bulk transition. As a result, the accumulation curve does not show saturation as τ approaches 1.

TABLE 1: Rate Constants and Parameters of Eq 1

k_2 (M^{-2} s^{-1})	2×10^6	A_0(M)	0.31
k_3 (M^{-2} s^{-1})	2.0	B (M)	0.3
k_4 (M^{-1} s^{-1})	3×10^3	C (M)	0.004
k_5 (M^{-2} s^{-1})	33	h_0	0.35 or 0.75
k_{-5} (M^{-1} s^{-1})	4.2×10^6	q	0.7
k_6 (M^{-1} s^{-1})	1×10^8	D_X (cm^2 s^{-1})	1.5×10^{-5}
k_{-6} (M^{-1} s^{-1})	3.0	D_Z (cm^2 s^{-1})	2.0×10^{-6}
k_7 (M^{-1} s^{-1})	1.0		
k_8/k_{-7} (M^2)	1×10^{-5}		
k_9 (s^{-1})	3×10^{-6}		

Mathematical Model

A. Model of the BZ Reaction. We use here the simplified version of the model of the BZ reaction derived in ref 29. With the quasi-steady-state approximation for $[HBrO_2^+]$ and $[Br^-]$ the model takes the form

$$\frac{\partial X}{\partial t} = \frac{-k_2X + k_3A}{k_2X + k_3A}\left(qk_7k_8\frac{BZ}{k_8 + k_{-7}h_0(C - Z)} + k_9B\right) - 2k_4X^2 + k_5h_0AX - k_{-5}U^2 + D_X\Delta X$$

$$\frac{\partial Z}{\partial t} = k_6U(C - Z) - k_{-6}XZ - \frac{k_7k_8BZ}{k_8 + k_{-7}h_0(C - Z)} + D_Z\Delta Z \quad (1)$$

$$U = \frac{-k_6(C - Z) + [(k_6(C - Z))^2 + 8k_{-5}(2k_5h_0AX + k_{-6}XZ)]^{1/2}}{4k_{-5}}$$

Here $X = [HBrO_2]$, $Z = [Fe(phen)_3^{3+}]$, $U = [HBrO_2^+]$, $A = [HBrO_3] = h_0A_0/(h_0 + 0.2)$, $A_0 = [NaBrO_3]$, $B = [CH_2(COOH)_2] + [CHBr(COOH)_2]$, $C = Z + [Fe(phen)_3^{2+}]$, h_0 is the Hammett acidity function, Δ is the Laplacian operator, and D_X and D_Z are the diffusion coefficients of X and Z, respectively.

The rate constants and parameters used in the simulations, unless otherwise stated, are summarized in Table 1.

We employ zero flux boundary conditions and spatially uniform initial conditions which correspond to the bulk transition into the oxidized state.

B. Model of the Heterogeneous Particle. In this paper we deal with pacemakers which have a period of oscillation shorter than that of the bulk. A small particle can form such a pacemaker if a heterogeneous reaction on its surface results in a decrease of the oscillation period in the neighborhood of the particle. In general, the heterogeneous catalytic reactions can be different from those in the bulk. We have no direct data on mechanisms of heterogeneous catalysis in the BZ reaction. For sake of simplicity, we assume that adsorption on the surface does not change the mechanism but only the rate constant of one of the key steps of the BZ reaction. This assumption is in accord with at least two suggested mechanisms of heterogeneous catalysis. In one, adsorption on the surface energetically stabilizes the activated complex. In the second, adsorption increases the probability that the reactants will collide so as to form the activated complex.[30] Thus, we model the heterogeneous pacemaker as a small part of the medium with one altered rate constant k_i. We choose rate constant k_5, which determines the rate of the autocatalytic oxidation of ferroin by bromate. Moderate variations of this constant result in significant changes in the oscillation period.

A thin layer of BZ solution is well described by a two-dimensional model. We assume that the particle is a disc situated at the bottom of the layer and that thickness of the disc is much smaller than that of the layer. In this case diffusion

above the disc does not differ from that in the bulk, and we can assume uniform diffusion throughout the entire system.

C. Model of a Random Population of Pacemakers. We model the heterogeneous particles as small circles; the reactor is also circular as in the experiments. We assume that the density of particles within the reactor obeys a uniform distribution. The particle radii are chosen from the log-normal distribution

$$P(r) = \frac{1}{\sigma r\sqrt{2\pi}} \exp\left[-\frac{1}{2\sigma^2}\left(\ln\left[\frac{r}{r_0}\right]\right)^2\right] \qquad (2)$$

This distribution is found for powder particles produced in various physical processes.[31,32] We assume that the parameters of the distributions of the particles are independent of the reagent concentrations and do not vary in time or from one experiment to another.

We perform the simulations as follows: (1) From a uniform random number generator we generate the spatial coordinates for 100 particles within a circle of the size of the experimental reactor. (2) The radius of each particle is obtained from a random number generator with a log-normal distribution according to eq 2 with $\sigma = 0.25$ and $r_0 = 15$ μm. (3) The dependence of the pacemaker oscillation period on the particle size is obtained from simulations of the deterministic reaction−diffusion system (1) with a single particle. We assume a fixed rate constant k_5 for all particles. (4) We assume that at time $t = 0$ the entire system undergoes a bulk transition from the reduced state to the oxidized state. The time of emergence of a circular wave from a particle i is equal to the oscillation period of the pacemaker formed by the particle: $t_i = T_P(r_i)$. However, a wave can be initiated only if the pacemaker is situated in a region which at time t_i is free of waves emitted earlier by other pacemakers. To check this condition for particle i, we calculate the distances R_{ij} from it to all other pacemakers that have already emitted waves and compare R_{ij} to the radii of those waves, $r_{ij} = v_j(t_i - t_j)$. Here v_j is the speed of the circular wave generated by particle j. Pacemaker i can generate waves only if $R_{ij} > r_{ij}$ for all j.

Methods of Computation

We use the CONT[33] numerical bifurcation and continuation package to calculate bifurcation diagrams of the point (well stirred) system corresponding to model (1).

We employ the finite-difference approximation to solve the reaction−diffusion equations (1). The corresponding system of ordinary differential equations is then solved with the LSODE subroutine,[34] using a numerically estimated Jacobian matrix. The numerical stability of the algorithm was improved as described in ref 35. Typical error tolerances are 1×10^{-7} relative and 1×10^{-12} absolute. Simulations are done on an IBM RISC 6000 workstation Model 340. We use, unless otherwise stated, 400 grid points for the 2 mm physical length.

Our system is two-dimensional. It is known that the circular wavefronts are stable to angular perturbations if the diffusion coefficient of the autocatalyst is larger than that of the inhibitor, which is true in our case. Therefore, we deal only with solutions that have radial symmetry, so we need only evaluate the radial component of the Laplacian operator.

Results of Simulations

A. Boundaries of the Oscillatory Domain of the Point System. In Figure 3 we have plotted the lines of supercritical Hopf bifurcation, which confine the oscillatory domain. Figure 3a shows the oscillatory domain in the h_0,B plane, and Figure 3b depicts this same region in the log(h_0),log(k_5) plane. In both planes, the top boundary separates the oscillatory domain from that of the oxidized steady state, and the bottom Hopf line is the boundary with the domain of the reduced steady state. The points that correspond to the experimental parameters of the bulk are shown in Figure 3 as solid circles. The points marked by squares and crosses in Figure 3b correspond to the parameters of the particles used in the simulations.

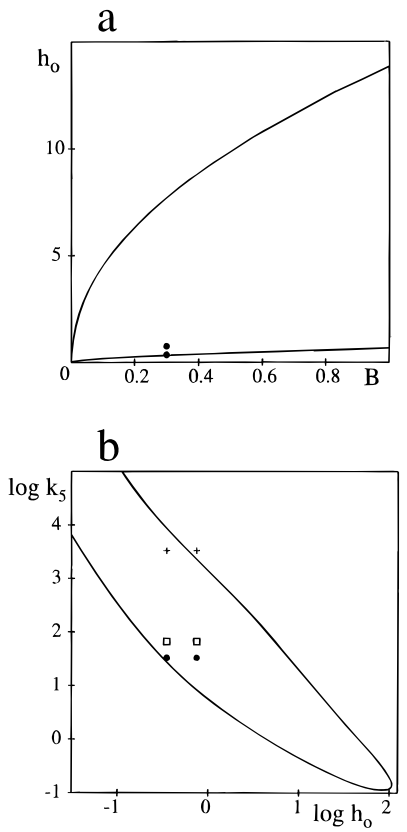

Figure 3. Bifurcation diagrams for model (1) in a well-stirred (point) system. (a) h_o,B plane; (b) log(k_5),log(h_o) plane. Solid circles - parameters of the bulk medium, squares - parameters of particles with $\Delta k_5 = 1.0$, crosses - parameters of particles with $\Delta k_5 = 99$.

B. Characteristics of Target Patterns. Power of a Pacemaker. It is obvious that characteristics of a pacemaker depends on both the particle area S and the parameter difference $(k_5^P - k_5^B)$, where k_5^P is the rate constant for the particle and k_5^B the rate constant for the bulk. One may expect that, in some parameter region, the characteristics of a pacemaker will depend only on the product $(k_5^P - k_5^B)S$. It is convenient to define the dimensionless "power" of a pacemaker, P, as

$$P = (k_5^P - k_5^B)S/k_5^B S_0 \qquad (3)$$

where the spatial scaling factor is $S_0 = D_x/(k_5 h_0 A)$. For k_5, D_x and A from Table 1 and $h_0 = 0.75$, we have $S_0 = 196$ μm^2. In what follows, we employ the relative difference in rate constants $\Delta k_5 = (k_5^P - k_5^B)/k_5^B$.

Figure 4 shows the dependence of the relative shift of pacemaker oscillation period T_P on P when Δk_5 varies at the constant particle size, and *vice versa*. One can see that the curves almost coincide when P is in the range 0−6. In the following simulations, we keep Δk_5 constant and vary the size of the particle.

Phase and Trigger Waves from Pacemakers. Both trigger and phase waves can form target patterns in oscillatory media.[9−12,36] Trigger and phase waves are the limiting cases

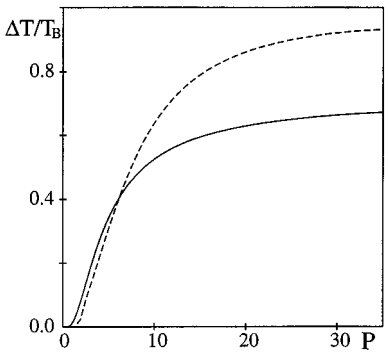

Figure 4. Shift in the oscillation period ($\Delta T = T_P - T_B$) as a function of the power of the pacemaker *P*. Solid line, constant $\Delta k_5 = 1.0$ and variable radius of the particle; dashed line, constant radius of the particle $r = 20$ μm and variable Δk_5. Power of the pacemaker is evaluated from eq 4.

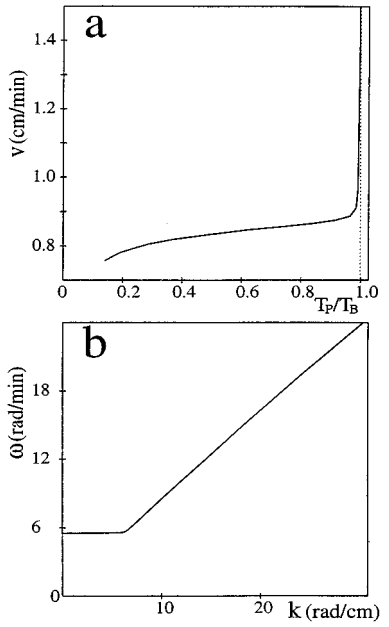

Figure 5. Dispersion curves for waves in model (1): a, dependence of the speed on the relative period of the wave; b, frequency vs wavenumber. The curves are calculated for the high acidity case.

when respectively the oscillation periods of pacemakers are much shorter than those of the bulk oscillations or very close to the latter. Aliev and Biktashev[37] propose employing the inflection point on the dispersion curve to separate the domains of trigger and phase waves.

Figure 5a shows the dependence of the stationary speed of a periodic wave train on the relative period of oscillations for model (1). In Figure 5b we plot the oscillation frequency versus the wave number. There is a region of slow trigger waves with speed almost independent of the oscillation period. This region is clearly separated from that of phase waves with the frequency very close to that of the bulk.

The dispersion curves shown in Figure 5 are calculated for the one-dimensional system, which corresponds to plane waves in two dimensions. The latter are a limiting case of circular waves whose speed depends on the curvature of the front. However, our simulations show that curvature effects for model (1) are essential only when the radius of the wave is less than 150 μm. The area covered by 100 circles with radius 150 μm is only 0.2% of the total area of our reactor. Therefore, the dispersion curves may be used to approximate the speed of the circular waves emanating from the pacemakers in our statistical simulations.

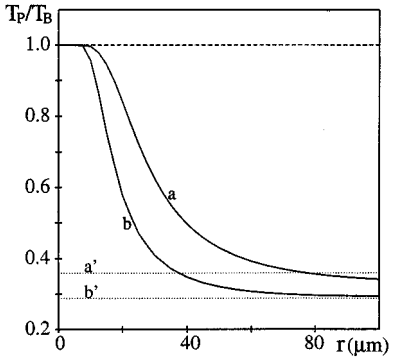

Figure 6. Dependence of the relative period of oscillations of the pacemaker (T_P/T_B) on the particle radius in model (1): $\Delta k_5 = 1.0$; a, low acidity; b, high acidity. Dotted lines show limits corresponding to homogeneous system with $k_5B = k_5P$ for the two acidities.

Dependence of the Pacemaker Period on Acidity. Our experimental data show that the density of target patterns increases strongly when the bromate concentration or the acidity of the solution increases.[3,20,22] The key terms of model (1) contain the product of these two parameters, and their effects on the dynamics of the system are almost equivalent. We have chosen to vary the acidity in our simulations.

Figure 6 shows the dependence of the relative oscillation period of the pacemaker (T_P/T_B) on particle size with $\Delta k_5 = 1.0$, calculated for two different acidities. For particle radii less than 10 μm, the relative period of oscillation is very close to 1, resulting in phase waves (Figure 5a). A larger difference in the oscillation periods, $T_P - T_B = \Delta T$, is required for trigger waves. The acidity has a large effect on the relative shift of the oscillation period, $\Delta T/T_B$, when the radius of the pacemaker is in the range 15−50 μm. As we show later, this difference in $\Delta T/T_B$ is responsible for the different kinetics of emergence of the circles at different acidities.

The dotted lines in Figure 6 indicate the asymptotic periods of oscillation for the homogeneous systems with $k_5^B = k_5^P$; the corresponding point systems are shown in Figure 3b as squares. At high acidity, the pacemaker period is always longer than the asymptotic period; at low acidity, the pacemaker period is shorter if the particle radius exceeds 80 μm. This latter result seems paradoxical. However, we are dealing here with pacemakers whose characteristics are determined by the interaction of a catalytic particle with the medium. In this case, a pacemaker can be formed by a particle which in isolation would be in a nonoscillatory state.

We employ $k_5^P = 100k_5^B$ to demonstrate that frequency of a pacemaker can differ dramatically from that of the point system corresponding to the particle. The positions of the point systems are marked by crosses in Figure 3b. At acidity $h_0 = 0.75$, the system is in the oxidized steady state, at $h_0 = 0.35$, the system oscillates with a high frequency, 2.9 Hz. Figure 7 shows the results of simulations for the two acidities. In the simulations we use 400 grid points for size of the system from 0.2 to 1.6 mm, while keeping constant number of 10 grid points for the pacemaker. The pacemaker has the minimal period of oscillations when radius of the particle equals 2 μm for high acidity and 3 μm for low acidity. The curves are similar for both cases what shows that difference in average rates of reactions between the particle and the bulk, can play more important role than the difference in the oscillation periods.

Kinetics of Emergence of Circles. Our experimental data show that the density of circles and target patterns increases with h_0. The dynamics of accumulation of the circles differs for the high and low acidity cases. Our model shows that the

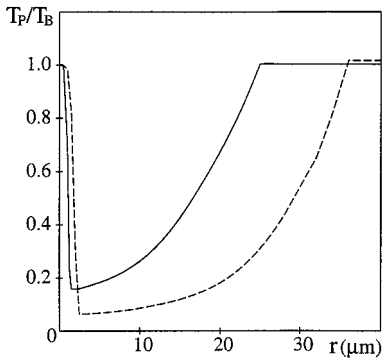

Figure 7. Dependence of the pacemaker period of oscillations on the particle radius - model (1), $\Delta k_5 = 99$. Solid line, high acidity; dashed line, low acidity.

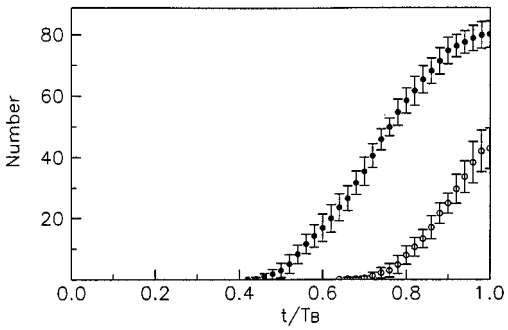

Figure 8. Cumulative plot of emergence of circular waves in the BZ reaction−diffusion system - model (1) for $\Delta k_5 = 1.0$ and log-normal distribution of particle sizes. Parameters of distribution: $\sigma = 0.25$, $r_o = 15\ \mu$m. Empty circles, low acidity ($h_o = 0.35$ M); solid circles, high acidity ($h_o = 0.75$ M). Bars indicate standard deviations.

oscillation period of the pacemaker formed by a particle of a given catalytic power depends strongly on the acidity of the medium. The overall pattern dynamics depends on the interaction of the randomly distributed particles.

To simulate the kinetics of circle appearance, we employ a stochastic model with pacemaker characteristics obtained from the above simulations. We assume the speed of the trigger waves is constant and neglect transient processes. This simplification results in an error of less than 5% in the average speed of circular wave spreading.

In order to compare the results of the experiments with those of the stochastic model, each simulation was repeated 10 times for both the high acidity and the low acidity cases for each set of parameters in the random distributions.

Figure 8 presents the calculated kinetics of accumulation of the circles. Comparison of the simulations with the experimental data (Figure 2) shows that the major properties, such as the numbers of circles and target patterns in the lower and higher acidity media, the relative time of appearance of the first circle, and the shapes of the curves, are similar.

Discussion

The aim of this study is to check whether the accepted mechanism of the BZ reaction can explain, at least in principle, the strong dependence of the density of target pattern centers on the reagent concentrations. Our statistical model contains a number of assumptions that are simple and reasonable, though not based on direct experimental data. To check the principal qualitative results of our simulations, we have performed a limited experimental study. For this study we employ unfiltered solutions prepared from commercial reagents, which are known to contain solid particle contaminants. We consider such source of a random heterogeneous contamination the most appropriate at this stage of our knowledge of the mechanisms of spontaneous target pattern formation in the BZ systems. It has been shown that filtering the working solutions can prevent formation of target patterns in excitable BZ media, but not in oscillating ones.[6,22,25] In the latter case the nonuniformities which produce the target patterns can be small particles that pass through the filter, defects in the reactor surfaces, or microbubbles of CO_2. In unfiltered solutions of commercial reagents, we can assume that most pacemakers are formed by solid particles that contaminate the reagents and thus employ a model of a single population of particles. In thoroughly filtered solutions we would need to consider at least three different populations of microheterogeneities and the possibility that a significant portion of the circles emerge as a result of homogeneous concentration fluctuations.

Both trigger and phase waves can be generated simultaneously by pacemakers with different periods of oscillations in a reaction−diffusion system with stiff local dynamics. The periods of the phase waves differ only slightly from the period of the bulk oscillations. In our case, the periods of the phase waves are longer than $0.95T_B$ (Figure 5a). As a result, in a population with a wide distribution of pacemaker frequencies, trigger waves will dominate.

We have simulated here only the kinetics of emergence of the pacemakers. Interaction between existing pacemakers leads to entrainment of the slower ones by the faster ones. As a result, after some time the total number of pacemakers starts to decrease, the distribution shifts toward shorter periods, and eventually only one, the fastest pacemaker, survives. Hence, instantaneous distributions of pacemakers depend significantly on time and are less convenient for comparison of simulations with experiment.

We have shown that the relative shift of the pacemaker period of oscillations $\Delta T/T_B$ depends strongly on the concentrations of the initial reagents. This explains the strong dependence of the density of target patterns on these concentrations. It also explains the absence of patterns near the boundaries of the oscillatory domain.[20,22] Our calculations show that closer to the boundary, $\Delta T/T_B$ is smaller than in the central part of the oscillatory domain. In the latter case, "powerful" catalytic particles form pacemakers with large $\Delta T/T_B$ that generate slow, short trigger waves; in the vicinity of the boundary the same particles give birth to pacemakers with small $\Delta T/T_B$ which emit fast, long phase waves. In the first case, the wavelength can be much shorter than the linear size of the reactor; in the second case, it can be much longer. Far from the oscillatory boundary, target patterns develop, while near the boundary, there are only small phase shifts along the reactor. If one follows the spatially averaged concentrations, then in the first case the observable oscillations will be strongly reduced in amplitude, while in the second case the observed oscillations will be nearly indistinguishable from the bulk oscillations.

We have studied here a specific case of local variation of the system parameters, namely, variation of the rate constants. It is evident from the law of mass action that local variations in the concentrations of the reservoir species will result in the same effect as variations of the rate constants. Thus, our results imply that, when the oscillations in the well-stirred system are stable, the corresponding bulk oscillations in an extended system can be stable or unstable to small local variations of the kinetic parameters, depending on the average values of the parameters, a finding in agreement with experimental observation.[20,22,27,28]

Acknowledgment. We gratefully acknowledge the support of the National Science Foundation Chemistry Division and the W. M. Keck Foundation.

References and Notes

(1) Zaikin, A. N.; Zhabotinsky, A. M. *Nature* **1970**, *225*, 535.
(2) Zhabotinsky, A. M.; Zaikin, A. N. In *Oscillating Processes in Biological and Chemical Systems II*; Sel'kov, E. E., Ed.; Nauka: Puschino; 1971; p 279.
(3) Zhabotinsky, A. M.; Zaikin, A. N. *J. Theor. Biol.* **1973**, *40*, 45.
(4) Orbán, M. *J. Am. Chem. Soc.* **1980**, *102*, 4311.
(5) De Kepper, P.; Epstein, I. R.; Kustin, K.; Orbán, M. *J. Phys. Chem.* **1982**, *86*, 170.
(6) Field, R. J., Burger, M., Eds. *Oscillations and Traveling Waves in Chemical Systems*; Wiley: New York, 1985.
(7) Ross, J.; Müller, S. C.; Vidal *C. Science* **1988**, *240*, 460.
(8) Kurin-Csörgei, K.; Szalai, I.; Körös, E. *React. Kinet. Catal. Lett.* **1995**, *54*, 217.
(9) Tyson, J. J.; Fife, P. C. *J. Chem. Phys.* **1980**, *73*, 2224.
(10) Hagan, P. S. *Adv. Appl. Math.* **1981**, *2*, 400.
(11) Kopell, N. *Adv. Appl. Math.* **1981**, *2*, 389.
(12) Kopell N.; Howard, L. N. *Stud. Appl. Math.* **1981**, *64*, 1; *Adv. Appl. Math.* **1981**, *2*, 417.
(13) Vasilyev, V. A.; Zaikin, A. N. *Kinet. Catal. (Russ.)* **1976**, *17*, 903.
(14) Zaikin, A. N.; Kawczynski, A. L. *J. Nonequilibr. Thermodyn.* **1977**, *2*, 39.
(15) Kobayashi, R.; Ohta, T.; Hayase, Y. *Phys. Rev. E* **1994**, *50*, R3291.
(16) Zhabotinsky, A. M.; Dolnik, M.; Epstein, I. R. *J. Chem. Phys.* **1995**, *103*, 10306.
(17) Sakaguchi, H. *Prog. Theor. Phys.* **1992**, *87*, 241.
(18) Mikhailov, A. S. *Physica D* **1992**, *55*, 99.
(19) Borckmans, P.; Dewel, G.; De Wit, A.; Walgraef, D. In *Chemical Waves and Patterns*; Kapral, R.; Showalter, K., Eds.; Kluwer: Dordrecht, 1995; p 323.
(20) Vidal, C.; Pagola, A; Bodet, J. M.; Hanusse, P.; Bastardie, E. J. *J. Phys.* **1986**, *47*, 1999.
(21) Pagola, A.; Vidal, C. *J. Phys. Chem.* **1987**, *91*, 501.
(22) Vidal, C. *J. Stat. Phys*. **1987**, *48*, 1017.
(23) Vidal, C.; Pagola, A. *J. Phys. Chem.* **1989**, *93*, 2711.
(24) Nagashima, H. *J. Phys. Soc. Jpn.* **1991**, *60*, 2797.
(25) Tyson, J. J. *J. Chim. Phys.* **1987**, *84*, 1359.
(26) Zhang, Y.-X.; Foerster, P.; Ross, J. *J. Phys. Chem.* **1992**, *96*, 8898.
(27) Zhabotinsky, A. M. In *Oscillating Processes in Biological and Chemical Systems*; Frank, G. M., Ed.; Nauka: Moscow, 1967; p 252.
(28) Zhabotinsky, A. M. In *Biological and Biochemical Oscillators*; Chance, B., et al., Eds.; Academic Press: New York, 1973; p 89.
(29) Zhabotinsky, A. M.; Buchholtz, F.; Kiyatkin, A. B.; Epstein, I. R. *J. Phys. Chem*. **1993**, *97*, 7578.
(30) Masel, R. I. *Principles of Adsorption and Reaction on Solid Surfaces*; Wiley: New York, 1996.
(31) Irani, R. R.; Callis, C. F. *Particle Size: Measurement, Interpretation and Application*; Wiley: New York, 1963.
(32) Mills A.; Davies, H. L.; Garley, M. S. *J. Chem. Soc., Faraday Trans.* **1990**, *86*, 2163.
(33) Marek, M.; Schreiber, I. *Chaotic Behavior of Deterministic Dissipative Systems*; Cambridge University: Cambridge, 1991.
(34) Hindmarsh, A. C. ODEPACK, a systematized collection of ODE solvers. In *Scientific Computing*; Stepleman, R. S., et al., Eds.; North-Holland: Amsterdam, 1983; pp 55−64.
(35) Zhabotinsky, A. M.; Györgyi, L.; Dolnik, M.; Epstein, I. R. *J. Phys. Chem*. **1994**, *98*, 7981.
(36) Buchholtz, F.; Dolnik, M.; Epstein, I. R. *J. Phys. Chem.* **1995**, *99*, 15093
(37) Aliev, R. A.; Biktashev, V. N. *J. Phys. Chem.* **1994**, *98*, 9676.

JP961603T